THE ASTROPHYSICAL JOURNAL, 292:291–296, 1985 May 1

THE MICROWAVE STRUCTURE OF HOT CORONAL LOOPS

GORDON D. HOLMAN[1]
Laboratory for Astronomy and Solar Physics, NASA/Goddard Space Flight Center, Greenbelt, Maryland
AND
MUKUL R. KUNDU
Astronomy Program, University of Maryland, College Park
Received 1984 September 11; accepted 1984 November 5

ABSTRACT

The thermal cyclotron emission from model dipole magnetic loops is computed. It is shown that a simple, isothermal dipole loop can show a great deal of spatial and polarization structure at microwave frequencies. This structure is sensitive to the observation frequency and angle of observation. Two qualitatively distinct microwave loop structures can be distinguished: (1) "thin loop," observed as a string of independent microwave peaks, corresponding to different harmonics of the local electron gyrofrequency; and (2) "thick loop," the harmonics are merged, so that a more continuous microwave structure is observed. It is shown that the presence of an external plasma can result in a change in the observed mode of polarization along one leg of a loop, without a change in the sign of the line-of-sight magnetic field. Models such as these, along with high-resolution microwave and related observations, can provide an excellent diagnostic of the magnetic and plasma properties of coronal loops.

Subject headings: radiation mechanisms — Sun: corona — Sun: radio radiation

I. INTRODUCTION

It is now well established that the solar corona, far from being the homogeneous, plane-parallel atmosphere envisioned in early models, is made up of a highly inhomogeneous distribution of closed magnetic loops and open field regions (cf. Vaiana and Rosner 1978). These magnetic structures are known to play an important role in the physics of coronal heating and of solar flares. A major stepping stone to fully understanding the role of coronal structures in these phenomena, however, is in determining the physical properties of the structures, particularly the strength and configuration of the confining magnetic field. Magnetograms give information about photospheric magnetic fields, but they do not yield direct information about magnetic fields in the corona. Coronal microwave emission, on the other hand, is known to be sensitive to the strength and orientation of the magnetic field in the radiating region (e.g., Kundu *et al.* 1977; Alissandrakis and Kundu 1982). Estimates of magnetic field strengths in active regions have been obtained from recent VLA observations of the Sun (cf. Kundu 1982), and VLA maps are now available that clearly show loop structures at microwave frequencies (Kundu and Velusamy 1980; Lang, Willson, and Rayrole 1982; McConnell and Kundu 1983).

Although some more detailed information about magnetic loop structures has been deduced from VLA maps of active regions at two or three frequencies (Lang, Willson, and Gaizauskas 1983; Shevgoankar and Kundu 1984), in general such information about coronal structures has not been forthcoming. This is primarily because high-spatial-resolution observations at microwave frequencies, especially at more than one frequency, are still relatively rare, and because of a lack of theoretical models with which to compare the data. The computation of the microwave emission from model coronal loops is the topic of this paper.

[1] NAS/NRC Resident Research Associate.

Two radiation mechanisms, thermal gyroresonance (cyclotron) emission and thermal bremsstrahlung (free-free emission), are known to contribute to the nonflaring microwave emission from the Sun (Kundu 1965). Nonthermal gyrosynchrotron radiation, important in solar flares, may also contribute to the nonflaring emission, but at present this has not been established. Modeling the solar chromosphere, transition zone, and corona as a plane-parallel atmosphere, Zheleznyakov (1962) and Kakinuma and Swarup (1962) showed that the spectrum and polarization of the "slowly varying component" of microwave emission from active regions can be explained if the emission mechanism is thermal gyroresonance emission. More recently, Zheleznyakov and Zlotnik (1980) have shown that the thermal gyroemission from hot structures in the corona, such as coronal loops, will appear as discrete lines and rapid spectral-index changes in the microwave spectrum. In this paper we show that the thermal gyroemission from hot coronal loops will also show a great deal of spatial structure, and that this structure is sensitive to the frequency and angle of observation. These results show that microwave observations of this structure can provide an excellent diagnostic of the magnetic and thermal properties of coronal loops.

In this paper we demonstrate the major characteristics that are expected of microwave loops by computing the thermal cyclotron emission from simple two-dimensional, isothermal dipole loop models. The loop models are described in § II. The computations are described, and the numerical results presented, in § III. Our results are summarized and discussed in § IV.

II. THE LOOP MODELS

The loop models for which the microwave emission is computed are two-dimensional, with the observer in the plane containing the loop. Hence, the numerical results of § III will represent one-dimensional scans along the length of the loop. The magnetic field is taken to be a dipole field, so that the magnitude and direction of the magnetic field in Cartesian

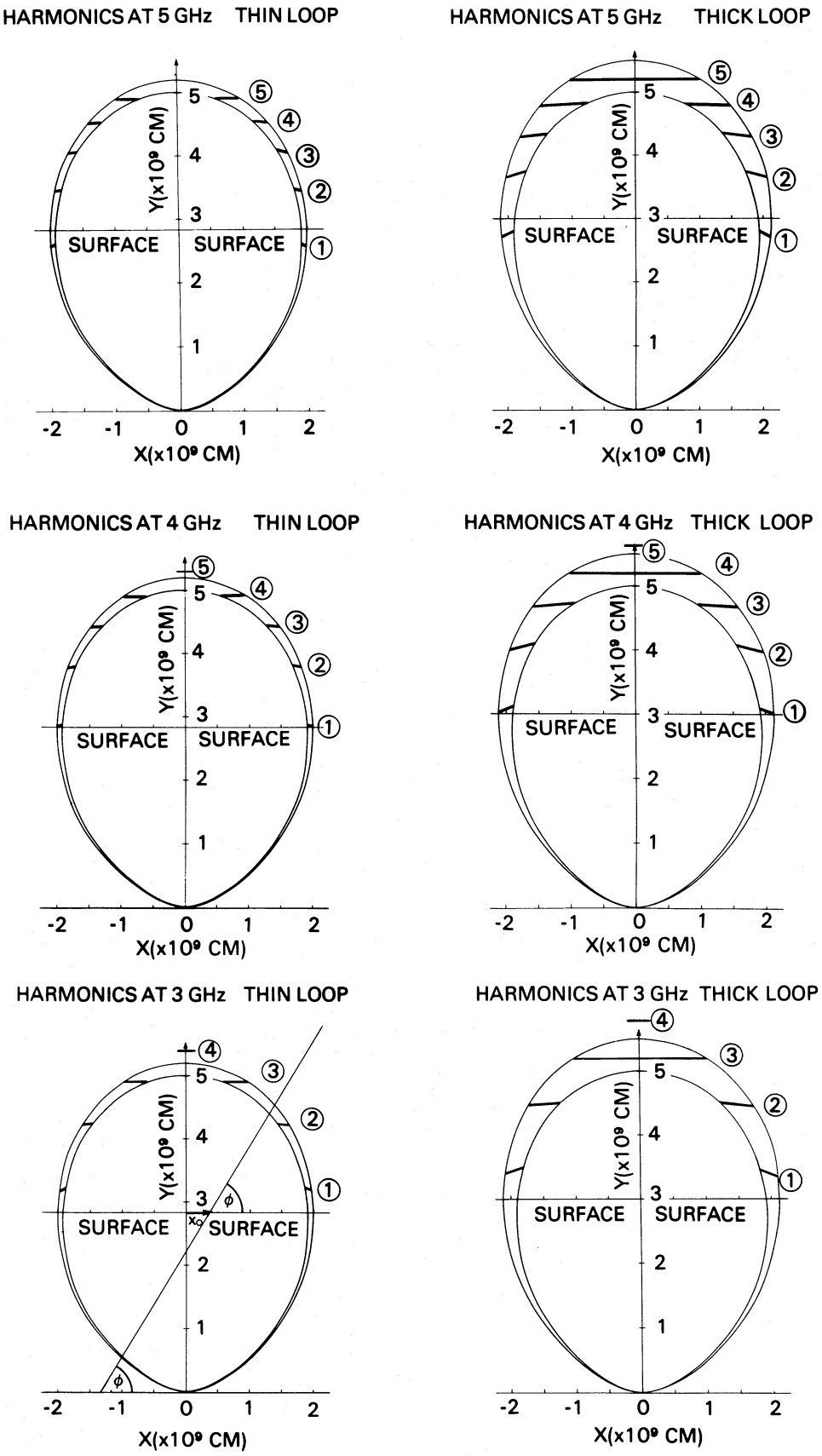

FIG. 1.—The thin and thick dipole-loop models. The heavy curves indicate locations within the loop where a harmonic (*circled number*) of the local electron gyrofrequency is equal to the indicated frequency of observation.

coordinates at position x, y is

$$|B| = B_U y_U^3 (4x^2 + y^2)^{1/2}/(x^2 + y^2)^2 , \quad (1a)$$

$$\tan\theta = 3xy/(2x^2 - y^2) , \quad (1b)$$

where B_U is the field strength at y_U, the highest point of the loop, and θ is measured from the x-axis. The loop is defined to exist between magnetic field lines that cross the y-axis at the points y_U and y_L, i.e.,

$$y_L y^2 < (x^2 + y^2)^{3/2} < y_U y^2 . \quad (2)$$

The solar "surface" is taken to be parallel to the x-axis, at the value of y for which the outermost field line of the loop becomes parallel to the y-axis. Therefore, the loop is restricted to the region

$$y > 0.545 y_U . \quad (3)$$

The loop geometry and magnetic field are completely determined by specifying the parameters y_L, y_U, and B_U.

The computations in the next section are all for models with $y_L = 5.0 \times 10^9$ cm and $B_U = 300$ G. Two values of y_U, 5.2×10^9 and 5.5×10^9 cm, are used. The loop models are shown in Figure 1. The loop with the lower value of y_U is labeled "thin loop," while the loop with the larger value of y_U is labeled "thick loop." Also shown within the loops are curves of constant magnetic field strength (*bold lines*) where the observation frequency is equal to a harmonic of the local electron gyrofrequency. Since the cyclotron radiation is emitted primarily in low harmonics of the gyrofrequency, these curves indicate the regions of the loop from which the cyclotron emission can be observed. The magnetic field strength at these locations is

$$B\,(\mathrm{G}) = 357 f\,(\mathrm{GHz})/n , \quad (4)$$

where f is the observation frequency and n is the harmonic number, shown circled in Figure 1.

The loops are taken to be isothermal, with $T = 3 \times 10^6$ K. The plasma density is taken to fall off exponentially with height:

$$n(y) = 1.0 \times 10^{11} \exp(-8.0 \times 10^{-10} y)\ \mathrm{cm}^{-3} . \quad (5)$$

This gives a density of approximately 10^9 cm^{-3} at the top of the loop and 10^{10} cm^{-3} at the base of the loop for both the thick and the thin loop models.

III. NUMERICAL RESULTS

The brightness temperature T_B and polarization of the microwave emission as a function of position along the projected length of the model loop are computed by numerically integrating the well-known solution (cf. Bekefi 1966) to the equation of radiative transfer along the observer's line of sight:

$$T_B^{X,O}(f, \phi, x_0) = \int_0^R T(l) \exp[-\tau_f^{X,O}(l)] \kappa_f^{X,O}(l) dl , \quad (6)$$

where

$$\tau_f^{X,O}(l) = \int_l^R \kappa_f^{X,O}(l') dl' \quad (7)$$

is the optical depth at position l, κ is the absorption coefficient, and the superscripts X, O refer to the extraordinary and ordinary modes of polarization. The absorption coefficient is a function of the local electron density, electron temperature (T), magnetic field strength, and the angle between the ray path and the magnetic field direction. Since gyroresonance absorption is significant only in the vicinity of harmonics of the local gyrofrequency (eq. [4]), the integrals in equations (6) and (7) need only be carried out in practice over the harmonics that contribute significantly to the absorption. The equations of Kai (1965) (see also Takakura and Scalise 1970) were used for the absorption coefficient in the computations presented here. The percentage polarization of the emission is simply

$$\text{polarization (\%)} = \frac{T_B^X - T_B^O}{T_B^X + T_B^O} \times 100 . \quad (8)$$

The line of sight is specified by its point of intersection with the solar "surface", x_0, and the angle between the line of sight and the surface (or equivalently, the x-axis), ϕ (see Fig. 1). When $\phi = 90°$, $x_0 = x$ and the line of sight is parallel to the y-axis.

Computed values of the brightness temperature and polarization as a function of x_0 for both the thin- and thick-loop models are shown in Figure 2 for $\phi = 90°$. The results are shown for three observation frequencies, 5, 4, and 3 GHz; the circled numbers indicate how the emission features correspond to the harmonic layers shown in Figure 1. Since the emission is symmetric around $x_0 = 0$, the emission from only half the loop is shown. (Note, however, that the observed polarization from the $x_0 < 0$ half of the loop will be opposite to that from the $x_0 > 0$ half of the loop, since the line-of-sight magnetic field component changes sign at $x_0 = 0$.) Of primary interest are the high degree of structure of this emission in both intensity and polarization, and the sensitivity of this structure to observation frequency. In these models emission from harmonics through $n = 3$ is observable, and the fourth harmonic emission is generally intense enough to also be observable. Determination of the harmonic number for the emission from a position x_0 gives a direct measure of the magnetic-field strength at that point within the loop, and the brightness temperature of the optically thick emission gives a direct measure of electron temperature at that location within the loop. The important distinction between the thin- and thick-loop models is seen to be that for the thin loop the emission from different harmonics is well separated, while the emission from the different harmonics in the thick loop is merged together so that there is not a distinct peak in the emission for each individual harmonic. This difference can be seen from Figure 1 by drawing lines parallel to the y-axis through various values of x_0. For the thin loop the line of sight only intersects one harmonic within the loop for any value of x_0, while for the thick loop the line of sight intersects more than one harmonic as the line of sight is moved from one harmonic region to the next (i.e., the harmonics overlap along the line of sight). It is interesting that for the thick-loop model at 3 GHz the harmonics are beginning to separate, so that the emission is beginning to take on the characteristics of thin-loop emission.

An interesting feature of the thin-loop emission from harmonics that are optically thick in both modes of polarization is that the emission is highly polarized at the edge of the (unpolarized) harmonic emission. This occurs because the less-optically-thick ordinary-mode emission falls off more rapidly (increases less rapidly) than the extraordinary-mode emission as the harmonic leaves (enters) the edge of the loop. A less rapid falloff in temperature at the edge of the loop will decrease the computed degree of polarization, but such a feature is characteristic of these optically thick harmonics.

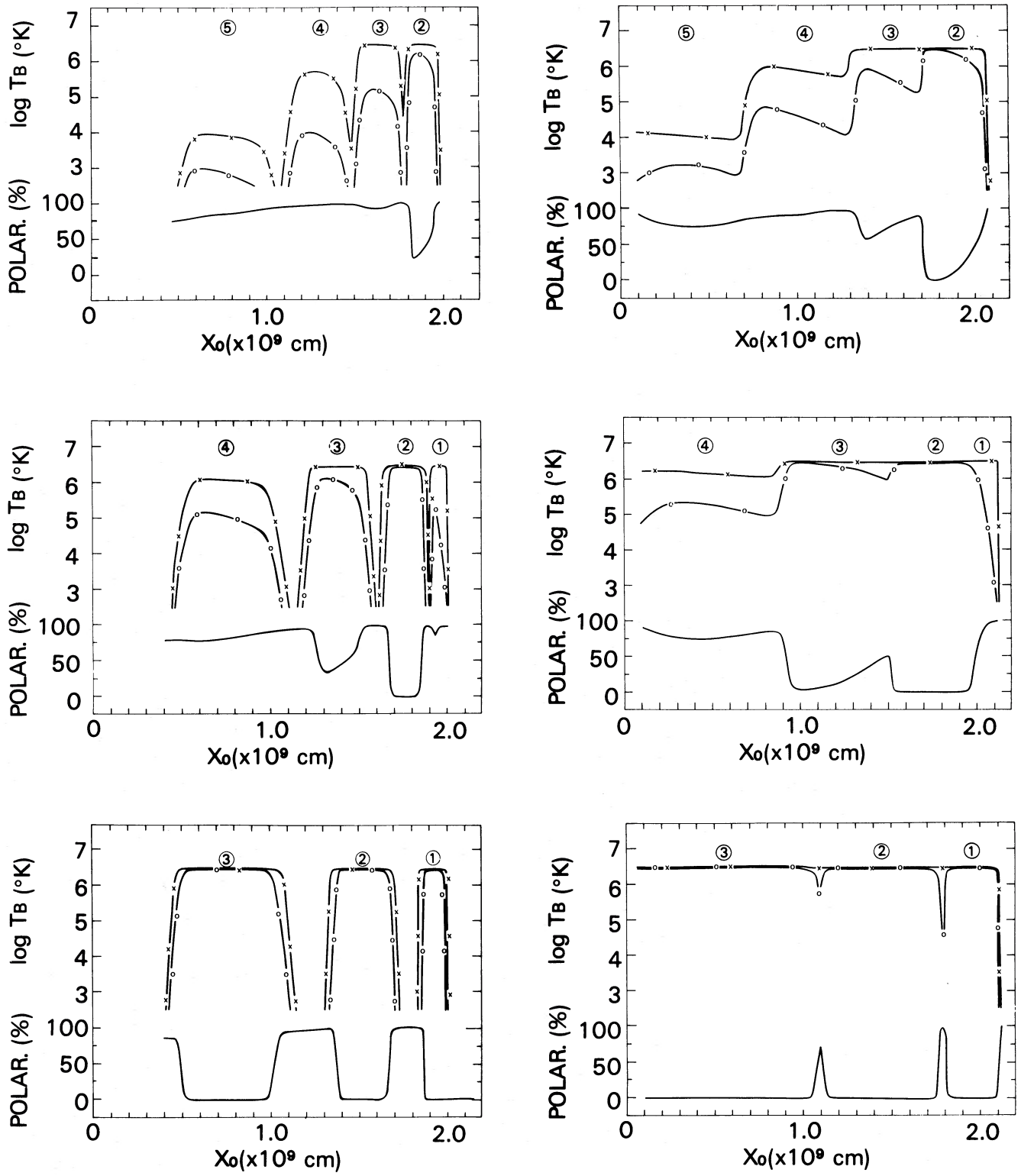

FIG. 2.—Brightness temperature and polarization as a function of position x_0 are plotted for the thin- and thick-loop models at three observation frequencies. On the curves, x denotes the extraordinary mode, o denotes the ordinary mode of polarization. Since the emission is symmetric about $x_0 = 0$, only half the loop is shown. Frequencies, top to bottom: 5, 4, 3 GHz; $\phi = 90°$ in each case; left col., thin-loop models, right col., thick-loop models.

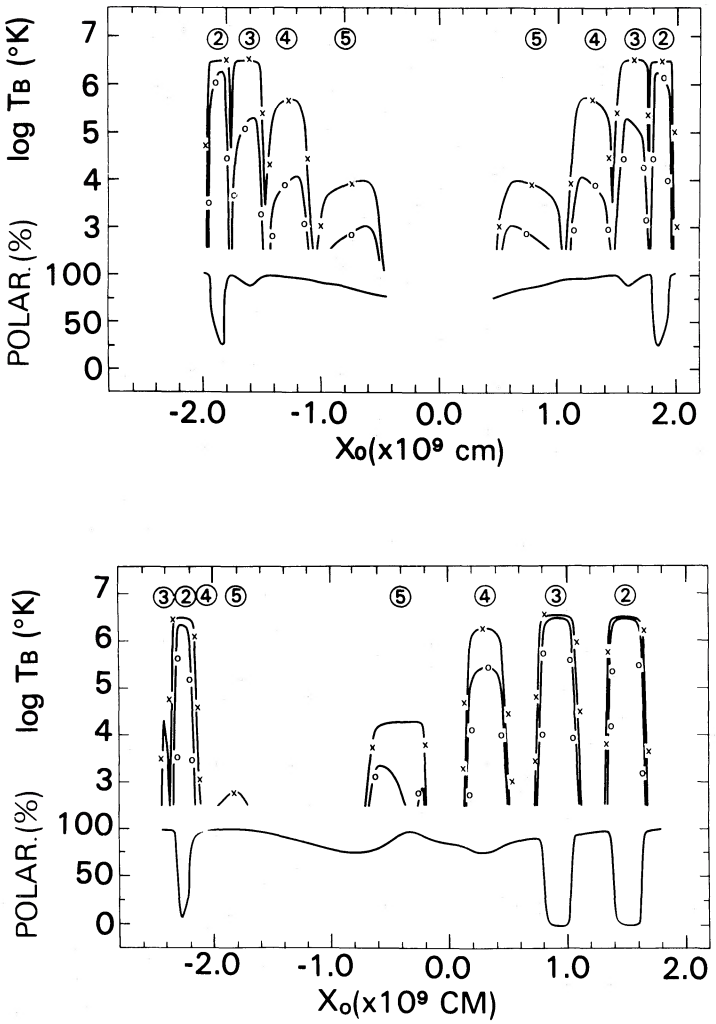

FIG. 3.—Thin-loop emission at 5 GHz for two angles of observation. *Top*. $\phi = 90°$; *bottom*, $\phi = 60°$.

Figure 3 shows a scan of the thin-loop model at 5 GHz with $\phi = 60°$. This is compared to the results for $\phi = 90°$. Since the results for $\phi = 60°$ are not symmetric around $x_0 = 0$, the entire loop is shown. The emission from the right ($x > 0$) half of the loop is seen to be more spread out, while that from the left half is more compressed. The ordering of the second and third harmonic emission from the left half of the loop is reversed, since the line of sight encounters the second harmonic region first as it scans to smaller values of x_0. The central part of the second and third harmonic emission from the right half of the loop is unpolarized, since the angle between the line of sight and the loop magnetic field θ is larger than for the $\phi = 90°$ case and, therefore, the absorption coefficient is greater, causing the ordinary-mode emission to be optically thick. The dip in the ordinary-mode emission at $x_0 = -0.3$ occurs where $\theta \approx 90°$. If this emission were intense enough to be observable, the observed polarization would reverse at this value of x_0 (from right to left, or vice versa). The dip in the third harmonic extraordinary-mode emission near $x_0 = -2.4$ occurs in a region where $\theta \approx 0°$. (It should be noted that although the results in these regions are qualitatively correct, the absorption coefficient used here is not accurate for $\theta \approx 90°$ or $\theta \approx 0°$.) A study of Figure 1 indicates how the emission will change for arbitrary values of ϕ. In particular, the emission from the thick-loop model will take on the characteristics of thin-loop emission for small enough values of ϕ.

The effects of adding an external 6×10^5 K plasma with the same density distribution as for the loop plasma (eq. [5]) are demonstrated in Figure 4. The thick-loop model with $\phi = 90°$ and $f = 4$ GHz is shown. (Note that the T_B scale is linear on this plot.) Other than lower polarization in general, the most notable effects are the reversal in polarization near $x_0 = 1.5$, where the second harmonic emission becomes dominant; and the complete absorption of the first harmonic loop emission by the external plasma. The polarization reversal occurs because of third harmonic absorption in the external plasma of the second harmonic extraordinary-mode emission. Since such a polarization reversal is usually interpreted to imply a change in the direction of the line-of-sight magnetic-field component, it is interesting that a polarization reversal can occur within the leg of a loop without implying such a field reversal. The percentage polarization near the reversal is not high ($\lesssim 50\%$), however, since the relatively high temperature of the external plasma limits the degree of polarization that can be attained. If this temperature were much lower, the opacity in the external plasma would not be high enough for the reversal to occur.

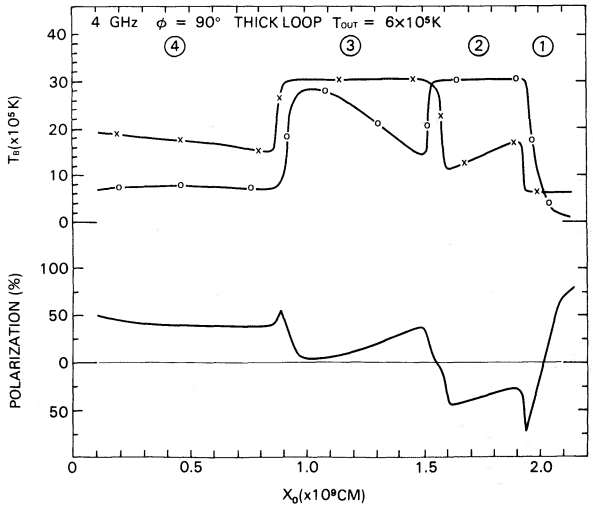

FIG. 4.—Thick-loop emission at 4 GHz with an external 6×10^5 K plasma (half loop).

Also, free-free absorption of the loop emission by this plasma would become more significant. Free-free absorption is, in fact, not completely insignificant for the parameters used here. At $x_0 \approx 1.9$, for example, where the effect upon the optically thick loop emission is greatest, the brightness temperature is reduced from that shown in Figure 4 by $\sim 20\%$. The important qualitative features of the emission are not affected, however.

IV. DISCUSSION AND CONCLUSIONS

The results obtained here demonstrate that even a simple isothermal dipole loop can show a great deal of spatial and polarization structure at microwave frequencies. This structure, and its sensitivity to frequency and angle of observation, can provide a powerful diagnostic of the magnetic and thermal properties of coronal loops. Arc-second–resolution maps at two or more observation frequencies can already be obtained with the VLA. Maps at closely spaced frequencies are best suited for comparison with models such as those presented here. Simultaneous high spatial resolution observations at EUV or soft X-ray energies would also be desirable, since these can provide information about the plasma density in the loop and an independent measurement of the plasma temperature. With observations such as these and further, more sophisticated, loop modeling, the possibility exists for mapping the strength and orientation of the magnetic field and the thermal plasma properties along the length of a coronal loop.

One obvious limitation of the models presented here is that they are two-dimensional, with the observer in the plane of the loop. Since this will not be the most common observational arrangement, and since instruments such as the VLA produce two-dimensional maps of the solar microwave emission, it is clearly desirable to produce theoretical maps from full three-dimensional models. Nevertheless, the two-dimensional models do demonstrate the important properties of the cyclotron emission from a looplike structure. A good idea of the full two-dimensional image that would be obtained by an observer not in the plane of the loop can, in fact, be obtained by comparing the numerical results obtained here with the drawings in Figure 1. In addition to the bonus of obtaining a projected loop shape, a feature that becomes immediately apparent is that the observer does not have to be very far out of the plane of the loop before the harmonics from the thick-loop model become separated, as for the thin-loop model.

As was mentioned in § 1, thermal bremsstrahlung can also contribute to the microwave emission from a coronal loop. For the loop models presented here, thermal bremsstrahlung is in fact negligible. Since the free-free opacity is proportional to $n^2/f^2T^{3/2}$, however, free-free emission does become important for higher density or lower temperature loops, or for lower observing frequencies. Hence, loop models must in general include both gyroresonance and free-free emission. Because of the density gradient in the loop, as the loop density is increased (or f or T decreased), bremsstrahlung first becomes important from the footpoints of the loop, and becomes important higher in the loop as n (f or T) is further increased (decreased). For these models, if n is increased or f further decreased, plasma suppression (i.e., the index of refraction) also becomes significant. (Plasma suppression is always significant for the first harmonic, extraordinary-mode emission. Since the optical thickness of the first harmonic is very large and the plasma frequency is relatively low for the models computed here, however, the first harmonic results obtained here are expected to be reasonably accurate.)

The authors thank Q. Yang for his assistance in developing the numerical code. G. Holman acknowledges support from the Laboratory for Astronomy and Solar Physics, NASA/Goddard Space Flight Center, and from the National Academy of Science's National Research Council. This work received partial support from NASA grants NGR 21-002-199 and NGL 21-002-033, NASA contract NSG 5320, and NSF grant ATM 81-03089.

REFERENCES

Alissandrakis, C. E., and Kundu, M. R. 1982, *Ap. J. (Letters)*, **253**, L49.
Bekefi, G. 1966, *Radiation Processes in Plasmas* (New York: Wiley).
Kai, K. 1965, *Publ. Astr. Soc. Japan*, **17**, 309.
Kakinuma, T., and Swarup, G. 1962, *Ap. J.*, **136**, 975.
Kundu, M. R. 1965, *Solar Radio Astronomy* (New York: Interscience).
———. 1982, *Rept. Progr. Phys.*, **45**, 1435.
Kundu, M. R., Alissandrakis, C. E., Bregman, J. D., and Hin, A. C. 1977, *Ap. J.*, **213**, 278.
Kundu, M. R., and Velusamy, T. 1980, *Ap. J. (Letters)*, **240**, L63.
Lang, K. R., Willson, R. F., and Rayrole, J. 1982, *Ap. J.*, **258**, 384.
Lang, K. R., Willson, R. F., and Gaizauskas, V. 1983, *Ap. J.*, **267**, 455.
McConnell, D., and Kundu, M. R. 1983, *Ap. J.*, **269**, 698.
Shevgoankar, R. K., and Kundu, M. R. 1984, *Ap. J.*, **283**, 413.
Takakura, T., and Scalise, E. 1970, *Solar Phys.*, **11**, 434.
Vaiana, G. S., and Rosner, R. 1978, *Ann. Rev. Astr. Ap.*, **16**, 393.
Zheleznyakov, V. V. 1962, *Soviet Astr.—A.J.*, **6**, 3.
Zheleznyakov, V. V., and Zlotnik, E. Ya. 1980, in *IAU Symp. 86, Radio Physics of the Sun*, ed. M. R. Kundu and T Gergely, (Dordrecht: Reidel), p. 87.

GORDON D. HOLMAN: NASA/Goddard Space Flight Center, Code 682, Greenbelt, MD 20771

MUKUL R. KUNDU: Astronomy Program, University of Maryland, College Park, MD 20742